Uhrf1 controls the self-renewal versus differentiation of hematopoietic stem cells by epigenetically regulating the cell-division modes

Jingyao Zhao[a,1], Xufeng Chen[a,1], Guangrong Song[b], Jiali Zhang[a], Haifeng Liu[a], and Xiaolong Liu[a,b,2]

[a]State Key Laboratory of Cell Biology, Chinese Academy of Sciences Center for Excellence in Molecular Cell Science, Institute of Biochemistry and Cell Biology, Shanghai Institutes for Biological Sciences, Chinese Academy of Sciences, Shanghai 200031, China; and [b]School of Life Science and Technology, ShanghaiTech University, Shanghai 200031, China

Edited by Ioannis Aifantis, New York University School of Medicine, New York, NY, and accepted by Editorial Board Member Tak W. Mak November 18, 2016 (received for review August 4, 2016)

Hematopoietic stem cells (HSCs) are able to both self-renew and differentiate. However, how individual HSC makes the decision between self-renewal and differentiation remains largely unknown. Here we report that ablation of the key epigenetic regulator Uhrf1 in the hematopoietic system depletes the HSC pool, leading to hematopoietic failure and lethality. Uhrf1-deficient HSCs display normal survival and proliferation, yet undergo erythroid-biased differentiation at the expense of self-renewal capacity. Notably, Uhrf1 is required for the establishment of DNA methylation patterns of erythroid-specific genes during HSC division. The expression of these genes is enhanced in the absence of Uhrf1, which disrupts the HSC-division modes by promoting the symmetric differentiation and suppressing the symmetric self-renewal. Moreover, overexpression of one of the up-regulated genes, Gata1, in HSCs is sufficient to phenocopy Uhrf1-deficient HSCs, which show impaired HSC symmetric self-renewal and increased differentiation commitment. Taken together, our findings suggest that Uhrf1 controls the self-renewal versus differentiation of HSC through epigenetically regulating the cell-division modes, thus providing unique insights into the relationship among Uhrf1-mediated DNA methylation, cell-division mode, and HSC fate decision.

Uhrf1 | HSCs | epigenetic regulation | cell-division mode | cell fate decision

Hematopoietic stem cells (HSCs) harbor the capacities of both self-renewal and differentiation to sustain life-long hematopoiesis (1). Although differentiation is responsible for producing all functional blood cells, self-renewal is critical in maintaining the size of the HSC pool (2). It has been reported that extrinsic cell signals, such as stem cell factor (SCF)/c-Kit signaling, Notch signaling, and Wnt signaling, contribute to the maintenance of HSC self-renewal (3–5). Moreover, the transcription factors Id2 (inhibitor of DNA binding 2) and Hoxa9 (homeobox A9) are required for HSC self-renewal and expansion (6, 7), and Hmga2 (high mobility group AT-hook 2) overexpression endows HSCs with higher self-renewal potential (8). Additionally, many transcription factors are involved in HSC differentiation. For example, the enforced expression of the erythroid master gene, Gata1 (GATA binding protein 1), in HSCs results in the exclusive generation of megakaryocyte and erythrocyte lineages (9). Consistently, Gfi1b (growth factor independent 1B), a downstream target of Gata1, controls erythroid and megakaryocytic differentiation by regulating TGF-β signaling (10). Recently, increasing research has focused on the functions of epigenetic regulation in HSCs. The absence of Dnmt1 (DNA methyltransferase 1) in HSCs impairs their self-renewal capacity (11, 12), whereas shortages of Dnmt3a and Dnmt3b block the differentiation process (13).

The self-renewal and the differentiation of HSCs were considered as two independent fate choices (14). Intriguingly, upon each division, HSCs undergo only one of the three mutually exclusive cell-division modes [symmetric self-renewal (SS), symmetric differentiation (SD), and asymmetric self-renewal (AS)] (15, 16), thus indicating that the regulation of HSC self-renewal cannot be separated from that of differentiation (17, 18). However, the key factors that regulate the HSC-division modes and the detailed mechanisms underlying how individual HSC accomplishes the decision of self-renewal versus differentiation remain largely unknown.

The epigenetic regulator Uhrf1 (ubiquitin-like, containing PHD and RING finger domains, 1) contains multiple functional domains that enable it to participate in various molecular processes (19–21). Among these processes, Uhrf1 is believed to be critical for maintaining DNA methylation (19). During DNA replication, Uhrf1 recognizes and binds to the hemimethylated CG residues generated at replication foci via the Set and Ring Associated domain, after which it recruits DNA methyltransferases and sustains the methylation of the newly synthesized DNA strand (22, 23). Previous research has reported that Uhrf1 facilitates the proliferation and maturation of colonic regulatory T cells (24), and our recent findings have suggested that Uhrf1 is required for invariant natural killer T cell development by regulating the Akt-mammalian target of rapamycin signaling pathway (25).

To investigate the functions of Uhrf1 in the hematopoietic system, we conditionally deleted Uhrf1 from hematopoietic cells. Uhrf1 deficiency leads to the exhaustion of the HSC pool and to a severe reduction in hematopoiesis. Uhrf1-deficient HSCs undergo erythroid-biased differentiation at the expense of self-renewal.

Significance

Hematopoietic stem cells (HSCs) harbor the capacities of both self-renewal and differentiation to sustain life-long production of all blood cells. However, how individual HSCs accomplish the decision of self-renewal versus differentiation remains largely unknown. Here, we find that Uhrf1, a key epigenetic regulator of DNA methylation, specifically controls this critical process. In the absence of Uhrf1, HSCs undergo erythroid-biased differentiation at the expense of self-renewal capacity, leading to hematopoietic failure and lethality. Mechanistically, Uhrf1 regulates the HSC-division mode by DNA methylation-mediated repression of the expression of certain erythroid-specific genes, and thus modulates the cell fate decision of HSCs. This study provides unique insights into the relationship among Uhrf1-mediated DNA methylation, cell-division mode, and HSC fate decision.

Author contributions: J. Zhao, X.C., and X.L. designed research; J. Zhao, X.C., G.S., J. Zhang, and H.L. performed research; J. Zhao, X.C., G.S., J. Zhang, and X.L. analyzed data; and J.Zhao, X.C., and X.L. wrote the paper.

The authors declare no conflict of interest.

This article is a PNAS Direct Submission. I.A. is a Guest Editor invited by the Editorial Board.

Data deposition: The data reported in this paper have been deposited in the Gene Expression Omnibus (GEO) database, www.ncbi.nlm.nih.gov/geo (accession no. GSE85450).

See Commentary on page 192.

[1]J. Zhao and X.C. contributed equally to this work.

[2]To whom correspondence should be addressed. Email: liux@sibs.ac.cn.

This article contains supporting information online at www.pnas.org/lookup/suppl/doi:10.1073/pnas.1612967114/-/DCSupplemental.

Notably, Uhrf1 plays essential roles in the establishment of DNA methylation patterns of differentiation-promoting genes during HSC division and in the regulation of HSC-division modes, and hence is critical for the decision of self-renewal versus differentiation of individual HSC. Altogether, our findings identified Uhrf1 as an essential regulator that controls the cell fate decision of individual HSC through epigenetically regulating the HSC-division modes.

Results

Uhrf1 Is Required to Maintain the Fetal Liver-HSC Pool. To study the function of Uhrf1 in hematopoiesis, we bred conditional Uhrf1$^{L/L}$ mice with the *Vav1-cre* strain. Uhrf1 was efficiently ablated from the hematopoietic system from 12.5 d postcoitum (dpc) mice (Fig. S1 *A–D*). Weaned *Vav1-cre*$^{+}$Uhrf1$^{L/L}$ mice (designated Uhrf1$^{-/-}$ mice) were not observed and litters did not have Mendelian genotype ratios (Fig. 1*A*). However, perinatal Uhrf1$^{-/-}$ mice with normal morphology but pale bodies (Fig. 1*B*) were identified. Uhrf1-deficient mice showed a significant decrease in fetal liver (FL) cellularity (Fig. 1*C*), compared with their WT control littermates (Uhrf1$^{L/L}$ or Uhrf1$^{L/+}$). Further analysis revealed a dramatic decrease in the absolute cell numbers of multilineage hematopoietic cells in the Uhrf1-deficient fetal liver (Fig. 1*D*).

These phenotypes inspired us to evaluate the roles of Uhrf1 in hematopoietic stem and progenitor cells. Consistent with the reduction in multilineage hematopoietic cells, Uhrf1-deficient fetal livers contained decreased megakaryocyte/erythroid progenitors (MEPs), common myeloid progenitors (CMPs), granulocyte-macrophage progenitors (GMPs), and common lymphoid progenitors (CLPs) (Fig. 1*E*). Moreover, Uhrf1-deficient mice displayed reduced hematopoietic stem/progenitor cells (HSPCs) [lineage^{-} cKit^{+} Sca1^{+} (LSK)] after 12.5 dpc (Fig. 1 *F* and *G*). Consistent with this result, FL-HSCs (CD150^{+} CD48^{-} Mac1^{low} LSKs) (26) also declined at 16.5 dpc (Fig. 1*H* and Fig. S2*A*). The aorta–gonad–mesonephros (AGM) region is a source of definitive HSCs before they colonize the fetal liver at 12.5 dpc (27). Notably, both the proportion and cell number of HSCs in the Uhrf1-deficient AGM were comparable to those in the control AGM at 11.5 dpc (Fig. S3 *A* and *B*). Together, these results indicate that Uhrf1 is required for the maintenance of the FL-HSC pool in the fetal liver.

Uhrf1 Is Essential for FL-HSC Self-Renewal. Given that the ablation of Uhrf1 in FL-HSCs results in HSC depletion, the survival and proliferation capacity of Uhrf1-deficient FL-HSCs was evaluated. Freshly isolated Uhrf1-deficient FL-HSCs showed similar levels of apoptosis compared with control FL-HSCs (Fig. 2 *A* and *B*), thus indicating that Uhrf1 deficiency did not impair the survival capacity of FL-HSCs. BrdU incorporation experiments were then performed to assess the proliferation capacity of FL-HSCs. Uhrf1-deficient FL-HSCs incorporated similar amounts of BrdU compared with control HSCs, a result suggesting that FL-HSCs can normally enter the cell cycle in the absence of Uhrf1 (Fig. 2 *C* and *D*). Collectively, these data show that Uhrf1-deficient FL-HSCs retain a normal survival and proliferation capacity.

We then wondered whether the defects in the establishment of the FL-HSC pool and in the consequential hematopoiesis resulted from the compromised self-renewal capacity of FL-HSCs in the absence of Uhrf1. To this end, we performed colony-forming unit (CFU) assays. The colonies formed by Uhrf1-deficient FL-HSPCs were much smaller than control colonies (Fig. 2*E*). Additionally, Uhrf1-deficient HSPCs formed more erythroid colonies (BFU-E) but fewer multilineage colonies (CFU-GEMM) and myeloid colonies (CFU-GM/G/M) compared with control HSPCs (Fig. 2*F*). Competitive bone marrow transplantations were then carried out to further analyze the self-renewal capacity of Uhrf1-deficient FL-HSCs. Uhrf1-deficient FL-HSPCs, compared with control FL-HSPCs, did not achieve multilineage reconstitution in irradiated mice (Fig. 2 *G* and *H* and Fig. S3 *C* and *D*). Moreover, Uhrf1-deficient FL-HSPCs could not reconstitute the HSC pool after transplantation (Fig. 2 *I* and *J*). Together, these data suggest that Uhrf1 is essential for FL-HSC self-renewal.

The HSC-Division Mode Is Impaired After Uhrf1 Ablation. Because the proliferation and survival of FL-HSCs remained unchanged in the absence of Uhrf1, cell fate analysis was performed to address whether HSC differentiation was affected. Notably, Uhrf1-de-

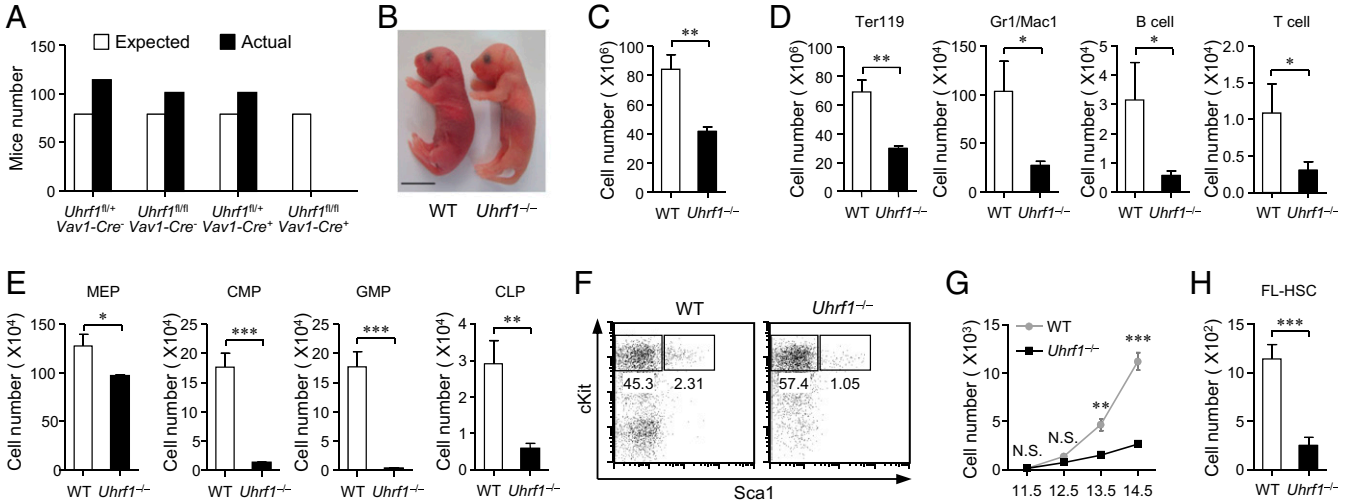

Fig. 1. Loss of Uhrf1 leads to embryonic lethality because of FL-HSC depletion. (*A*) Expected (according to Mendel's law) and actual weaned mouse numbers of different genotypes. (*B*) Representative images of control littermates and Uhrf1$^{-/-}$ mice at birth. (Scale bar, 1 cm.) (*C*) Cellularity of fetal livers from control littermates and Uhrf1$^{-/-}$ mice at 16.5 dpc ($n = 3$). (*D* and *E*) Absolute cell numbers of hematopoietic cells (*D*) and HPCs (MEPs, CMPs, GMPs, CLPs) (*E*) from control and Uhrf1-deficient fetal livers at 14.5 dpc ($n = 3$). (*F*) Flow cytometric analysis of HSPCs (lineage^{-} cKit^{+} Sca1^{+}, LSK) and HPCs (lineage^{-} cKit^{+} Sca1^{-}, LK) from control and Uhrf1-deficient fetal livers at 14.5 dpc. Lineage^{-} viable cells are shown. (*G*) Absolute cell numbers of HSPCs (LSKs) from control and Uhrf1-deficient fetal livers at different gestational ages ($n = 3$–4 for each genotype for each gestational age). (*H*) Absolute cell numbers of FL-HSCs (CD150^{+} CD48^{-} Mac1^{low} LSKs) from control and Uhrf1-deficient fetal livers at 16.5 dpc ($n = 3$). The data are means ± standard deviation, for all panels: *$P < 0.05$, **$P < 0.01$, ***$P < 0.001$ by Student's *t* test; N.S.: no significance.

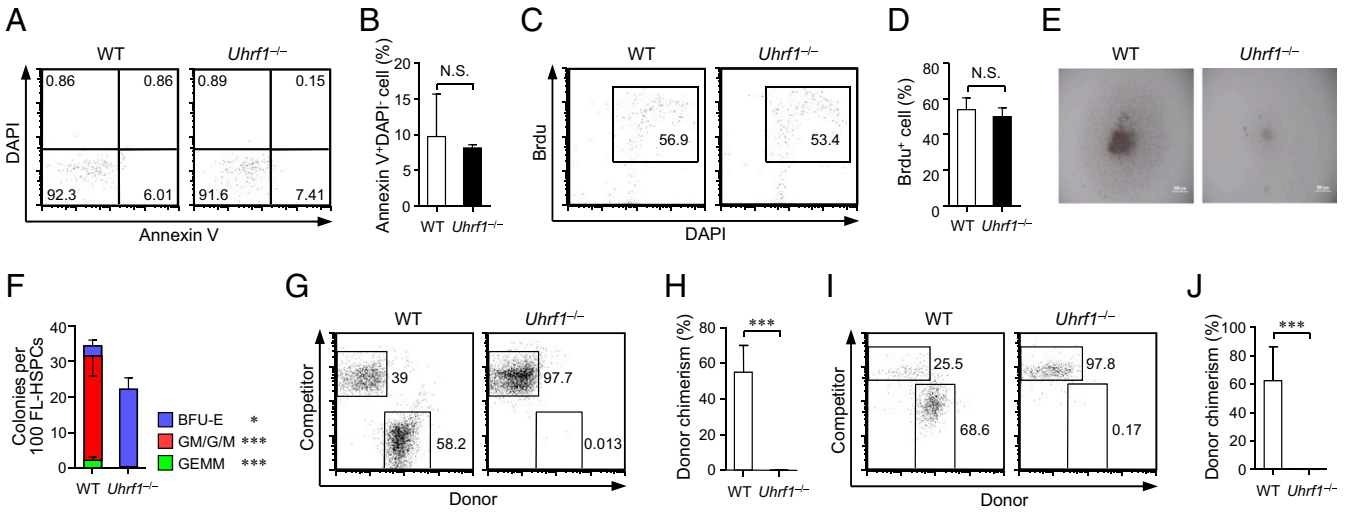

Fig. 2. Impaired FL-HSC self-renewal in the absence of Uhrf1. (*A* and *B*) Representative dot plots of the Annexin V staining profile (*A*) and the percentage of cells that undergo apoptosis (Annexin V$^+$ DAPI$^-$) (*B*) of control and Uhrf1-deficient FL-HSCs (CD150$^+$ CD48$^-$ LSKs) at 13.5 dpc ($n = 3$). (*C* and *D*) BrdU incorporation profiles (*C*) and the percentages of cells that entered the S phase (*D*) were assessed 2 h after BrdU injection ($n = 6$). (*E*) Representative images of colonies generated from control and Uhrf1-deficient FL-HSPCs (LSKs) at 13.5 dpc. Images were captured on day 10. (Scale bars, 500 μm.) (*F*) Numbers of multilineage colonies (CFU-GEMM), erythroid colonies (BFU-E), and myeloid colonies (CFU-GM/G/M) generated by 100 FL-HSPCs (LSKs) sorted from control and Uhrf1-deficient fetal livers at 13.5 dpc ($n = 3$). (*G* and *H*) Representative dot plots (*G*) and percentages (*H*) of donor chimerism of peripheral blood mononuclear cells (PBMCs) (8 wk) in recipients transplanted with 1,000 sorted FL-HSPCs (LSKs) from control or Uhrf1-deficient fetal livers at 13.5 dpc together with 500,000 competitor bone marrow cells (WT, $n = 9$; Uhrf1$^{-/-}$, $n = 8$). (*I* and *J*) Representative dot plots (*I*) and percentages (*J*) of donor chimerism of HSPCs (LSKs; 8 wk) in recipients transplanted as described above (WT, $n = 9$; Uhrf1$^{-/-}$, $n = 8$). The data are means ± standard deviation, for all panels: $^*P < 0.05$, $^{**}P < 0.01$. $^{***}P < 0.001$ by Student's *t* test; N.S.: no significance.

ficient FL-HSPCs could not sustain the HSPC pool, whereas more hematopoietic progenitor cells [HPCs (lineage$^-$ cKit$^+$ Sca1$^-$, LK), referred to as HPC(LK)s] were generated (Fig. 3 *A*–*C*). These results suggested that FL-HSPCs are more prone to undergoing differentiation when Uhrf1 is deleted.

Given that self-renewal and differentiation are coordinately regulated in HSCs through the exclusive choice among the three stem-cell division modes (SS, SD, and AS) during HSC division (15, 16), we then sought to determine whether the attenuated self-renewal and the increased differentiation is resulted from abnormal HSC-division modes. To address this possibility, we stained the cell-fate determinant Numb [numb homolog (*Drosophila*)] in individual Uhrf1-deficient and WT FL-HSPC and measured the ratios of SS divisions (low expression of Numb in both daughter cells), SD (high Numb expression in both daughter cells), and AS divisions (higher expression of Numb protein in one of two daughter cells) (Fig. 3*D*) (16, 17). Notably, significantly fewer SS divisions (25.82% ± 9.16% vs. 41.18% ± 3.93% in WT FL-HSPCs) and more SD divisions (46.15% ± 10.46% vs. 30.96% ± 8.12% in WT FL-HSPCs) were observed in Uhrf1-deficient FL-HSPCs (Fig. 3*E*). Consistently, Uhrf1-deficient FL-HSCs (CD150$^+$ CD48$^-$ LSKs) also underwent fewer SS divisions (31.77% ± 3.59% vs. 55.37% ± 4.33% in WT FL-HSCs) and more SD divisions (50.93% ± 2.04% vs. 26.36% ± 5.64% in WT FL-HSCs) (Fig. 3*F*). Moreover, *Numb* mRNAs were comparable between Uhrf1-deficient and control FL-HSCs, indicating that the up-regulation of Numb in the daughter cells was not as a direct consequence of Uhrf1 ablation (Fig. S3*E*). These findings suggested that Uhrf1 is involved in the regulation of HSC-division modes and controls the decision of self-renewal and differentiation of FL-HSCs.

To a lesser extent, some Uhrf1-deficient FL-HSCs still underwent SS and AS divisions (Fig. 3 *E* and *F*), thus raising the question of how the FL-HSC pool was depleted under such a division pattern. Therefore, we stained FL-HSPCs with the cell division indicator 5-(and 6)-Carboxyfluorescein diacetate succinimidyl ester (CFSE), and then assessed the maintenance of the HSC pool after division. The proportion of FL-HSPCs declined as cell divisions continued (28). Interestingly, Uhrf1-deficient FL-HSPCs declined faster than their WT counterparts, thus eventually leading to the depletion of the HSC pool after multiple rounds of division (Fig. 3 *G* and *H*).

Given that MEPs declined to a much lesser extent than CMPs, GMPs, and CLPs in Uhrf1-deficient fetal livers (Fig. 1*E*), and Uhrf1-deficient HSPCs formed excessive erythroid colonies in the CFU assays (Fig. 2*F*), we then sought to explore whether the increased differentiation potential of Uhrf1-deficient FL-HSCs was accompanied by biased lineage commitment. Notably, among those assessed progenitors, only MEP in Uhrf1-deficient fetal livers displayed an increased proportion compared with the WT control (Fig. 3 *I* and *J* and Fig. S3 *F* and *G*), suggesting that Uhrf1-deficient FL-HSCs underwent erythroid-biased differentiation.

FL-HSCs Up-Regulate Erythroid-Specific Gene Expression in the Absence of Uhrf1. To investigate the molecular mechanism of Uhrf1 in controlling the self-renewal versus differentiation of FL-HSCs, high-throughput sequencing was performed to analyze the transcriptomes of WT and Uhrf1-deficient FL-HSPCs. Consistent with the erythroid-biased differentiation of Uhrf1-deficient FL-HSCs (Fig. 3 *I* and *J*), genes involved in erythrocyte differentiation were significantly enriched in Uhrf1-deficient FL-HSPCs according to the Gene Ontology (GO) enrichment analysis. Although this cluster was ranked seventh among the top 24, with a score greater than 5, it was ranked first in the cell fate commitment category (Fig. 4*A* and Table S1). Gene-set enrichment analysis using gene sets from lineage-restricted progenitors defined by Sanjuan-Pla et al. (29) revealed that genes associated with myeloid and lymphoid (CLP) programming were enriched in WT HSPCs, whereas genes associated with erythroid progenitors (were enriched in Uhrf1-deficient HSPCs. Moreover, the HSC self-renewal associated genes defined by Krivtsov et al. (30) were enriched in WT HSPCs but not Uhrf1-deficient HSPCs (Fig. S4*A*). We then generated gene signatures specific for stemness of HSPCs (stem signature) or myeloerythroid progenitors (MEP signature) by subtracting the genes expressed in WT HPC(LK)s from those

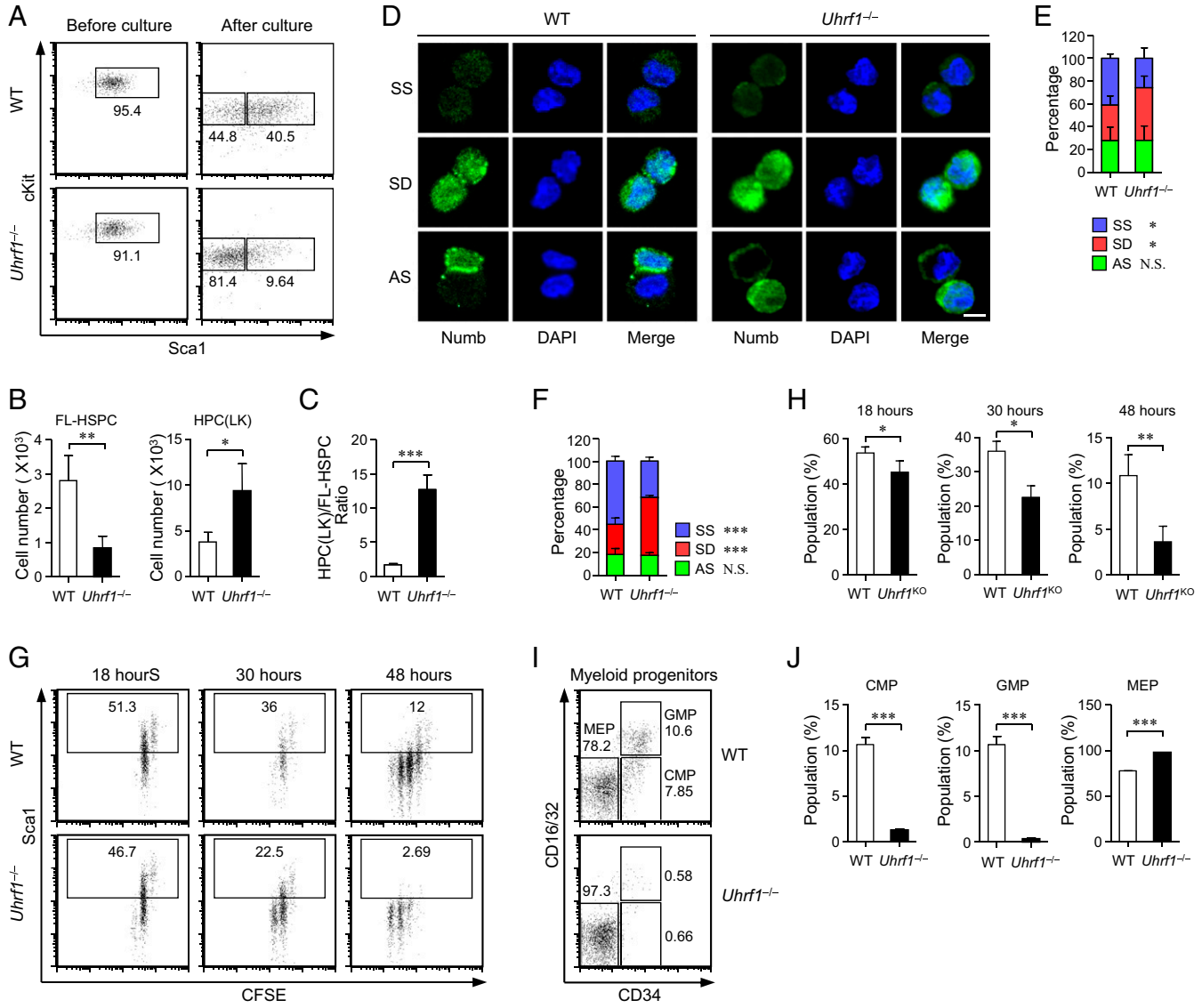

Fig. 3. Uhrf1 ablation promotes the symmetric differentiation and suppresses the SS of HSCs. (*A–C*) Analysis of the self-renewal capacity of FL-HSPCs in culture. Two-thousand sorted FL-HSPCs (LSKs) from control or Uhrf1-deficient fetal livers at 13.5 dpc were cultured in IMDM supplemented with 10% (vol/vol) FBS, 50 μM 2-mercaptoethanol, 50 ng/mL SCF, 10 ng/mL mIL-3, and 10 ng/mL mIL-6 for 40 h before flow cytometric analysis. (*A*) Representative dot plots of the FL-HSPCs (LSKs) and HPC(LK) proportions before (*Left*) and after (*Right*) culture are shown. (*B*) Absolute numbers of FL-HSPCs (LSKs) and HPC(LK)s yielded by control or Uhrf1-deficient FL-HSPCs (LSKs) in culture. (*C*) The ratios of HPC(LK) related to FL-HSPCs (LSKs) are shown ($n = 4$). (*D*) Staining of Numb (green) in sorted WT (*Left*) and Uhrf1-deficient (*Right*) FL-HSPCs (LSKs) after one division to identify SS (*Top*), SD (*Middle*), and AS (*Bottom*) division. DNA was counterstained with DAPI (blue). (Scale bar, 5 μm.) (*E*) Cell-division mode of control and Uhrf1-deficient FL-HSPCs (LSKs) ($n = 220$ (WT) or 214 (Uhrf1-deficient) cell doublets from five independent experiments). (*F*) Cell-division mode of control and Uhrf1-deficient FL-HSCs ($CD150^+$ $CD48^-$ LSKs) ($n = 143$ (WT) or 128 (Uhrf1-deficient) cell doublets from four independent experiments). (*G* and *H*) In vitro assessment of the maintenance of the HSPC (LSK) pool. Fetal liver cells from control or Uhrf1-deficient embryos at 12.5 dpc were stained with CFSE and cultured overnight in the presence of 10 ng/mL TPO and 100 ng/mL nocodazole before sorting. Sorted $CFSE^+$ FL-HSPCs (LSKs) were cultured for the indicated time periods before analysis of the maintenance of the HSPC (LSK) pool. Representative dot plots (*G*) and percentages of Lin^- $cKit^+$ population (*H*) of sorted $CFSE^+$ FL-HSPCs (LSKs) cultured for the indicated time points are shown ($n = 3$–5 for each time point). (*I* and *J*) Representative dot plots (*I*) and percentages (*J*) of myeloid progenitors in control and Uhrf1-deficient fetal livers at 14.5 dpc ($n = 3$). The data are means ± standard deviation, for all panels: $^*P < 0.05$, $^{**}P < 0.01$, $^{***}P < 0.001$ by Student's *t* test; N.S.: no significance.

expressed in WT FL-HSPCs or vice versa (12). Of the stem signature genes, 71.28% showed lower expression and 28.72% showed higher expression in Uhrf1-deficient FL-HSPCs compared with WT FL-HSPCs (Fig. 4*B*). Interestingly, among the MEP signature genes, genes enriched in erythroid differentiation (27.54%) were up-regulated in the absence of Uhrf1, whereas the remaining genes enriched in myeloid-specific genes (72.46%) were suppressed, consistent with previous research (9) (Fig. S4*B*). Particularly, in comparison with the WT control, Uhrf1-deficient FL-HSPCs up-regulated certain erythrocyte differentiation-related genes [e.g., *Gata1*, *Gata2* (GATA binding protein 2), *Gfi1b*, *Car1* (carbonic anhydrase 1), *Zfpm1* (zinc finger protein, multitype 1), and *Itga2b* (integrin alpha 2b)] (Fig. 4 *C* and *E*), most of which were physiologically up-regulated in HPC(LK)s (Fig. S4*C*), whereas some genes [*Id2*, *Satb1* (special AT-rich sequence binding protein 1), *Hmga2*] that play critical roles in HSC maintenance were down-regulated (Fig. 4 *C* and *D*). These results suggested that Uhrf1 controls the self-renewal versus differentiation of FL-HSCs by suppressing the expression of the erythroid-specific genes and maintaining the expression of HSC stemness genes.

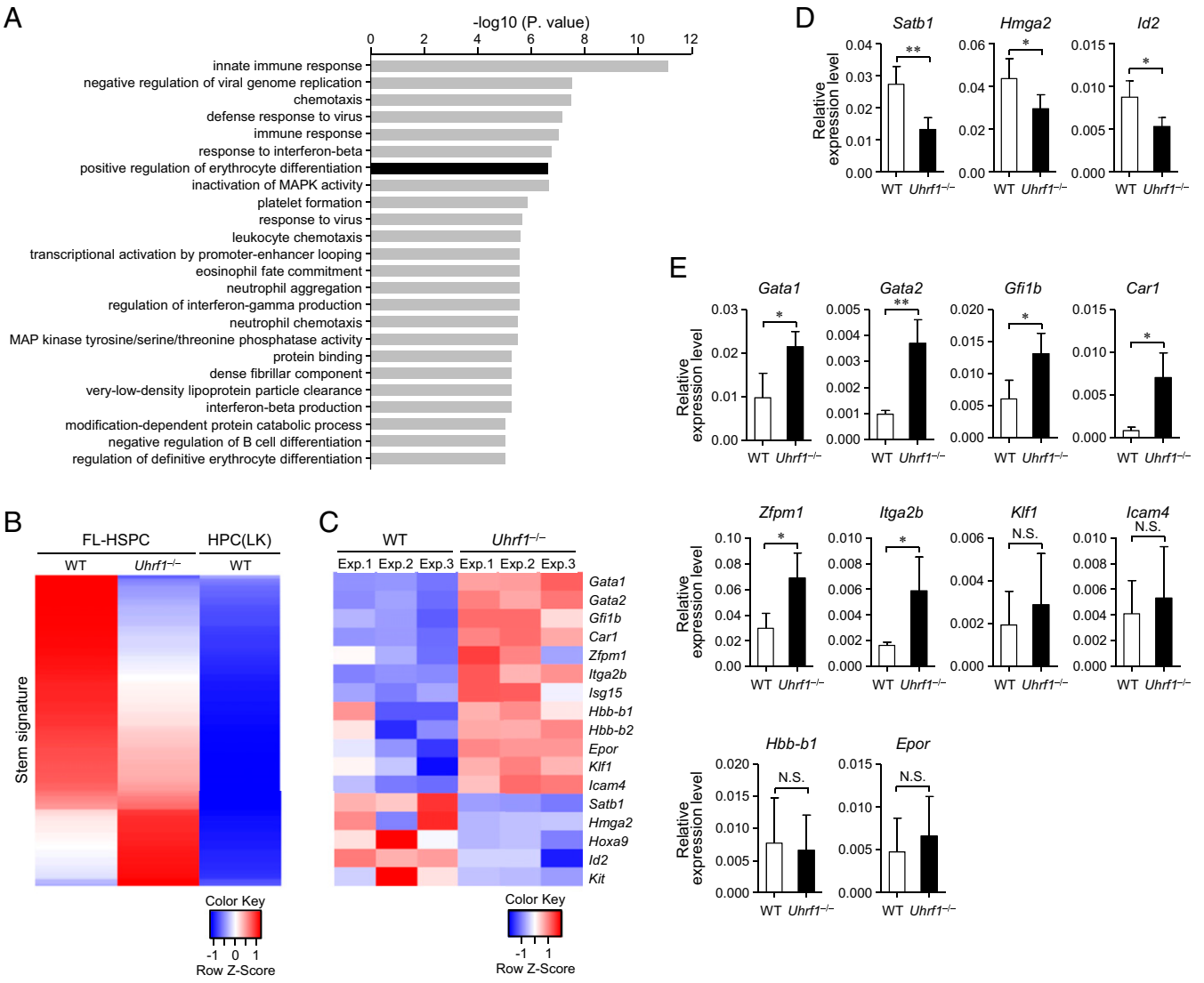

Fig. 4. Uhrf1-deficient FL-HSCs up-regulate a cluster of genes involved in erythroid development. (*A*) Pathway enrichment analysis of differentially expressed genes ($P < 0.05$, fold-change > 2.0) in FL-HSPCs (LSKs) from control and Uhrf1-deficient fetal livers. (*B*) Stem signature gene sets were generated by subtracting the genes expressed in WT HPC(LK)s from those expressed in WT FL-HSPCs (LSKs), as calculated from $P < 0.05$ and log fold-change > 2.0. Absolute expression values were transformed to *z*-scores before visualization. (*C*) Expression of representative genes with known functions in stem cells (*Satb1*, *Hmga2*, *Hoxa9*, *Id2*, *Kit*) and erythroid cells (*Gata1*, *Gata2*, *Gfi1b*, *Car1*, *Zfpm1*, *Itga2b*, *Isg15*, *Hbb-b1*, *Hbb-b2*, *Epor*, *Klf1*, *Icam4*). (*D* and *E*) Validation of the transcriptional levels of representative stemness genes (*D*) and erythroid genes (*E*) in FL-HSPCs (LSKs) from control and Uhrf1-deficient fetal livers ($n = 3$–5). The data are means ± standard deviation, for all panels: $^*P < 0.05$, $^{**}P < 0.01$ by Student's *t* test; N.S.: no significance.

Uhrf1 Coordinates the HSC-Division Mode with the DNA Methylation Patterns of Erythroid-Specific Genes. Uhrf1 has been reported to act by recruiting DNA methyltransferases to the newly synthesized DNA strand, thereby facilitating the maintenance of DNA methylation during cell division (19, 22). Indeed, Uhrf1-deficient HSPCs showed reduced global DNA methylation level compared with control HSPCs. (Fig. S5*A*). Notably, the methylation level of genes unrelated to hematopoiesis (e.g., *Ctla4*) remained unchanged after Uhrf1 ablation (Fig. S5 *B*–*D*). To further address whether Uhrf1 plays a role in the establishment of the DNA methylation patterns of erythroid-specific genes, we performed bisulfite sequencing to assess the DNA methylation levels of several up-regulated erythroid-specific genes in Uhrf1-deficient FL-HSPCs. The CpG sites around the transcription start sites of *Gata1*, *Gfi1b*, and *Car1*, which are critical for regulating the expression of these genes (11, 31, 32), showed decreased DNA methylation levels compared with those in WT controls (Fig. 5 *A* and *B*). This decreased methylation might lead to the increased expression of these genes in Uhrf1-deficient FL-HSPCs (Fig. 4 *C* and *E*). Moreover, we found that the CpG sites around the transcription start sites of several down-regulated stemness genes (*Satb1*, *Id2*) stayed almost as unmethylated in Uhrf1-deficient FL-HSPCs as those in WT controls (Fig. S5 *E* and *F*), suggesting that the down-regulation of these stemness genes is unlikely to be relevant to the DNA methylation regulations and may be the consequence of enhanced expression of multiple erythroid-specific genes.

We then wondered whether the DNA methylation levels of the erythroid-specific genes were progressively decreased through generations, given that the FL-HSC pool was exhausted after multiple rounds of cell division in the absence of Uhrf1 (Fig. 3 *G* and *H*). To address this possibility, the DNA methylation levels of the master erythroid-specific gene Gata1, as an example, were analyzed in FL-HSPCs from different cell generations. Indeed, the DNA methylation level of *Gata1* in Uhrf1-deficient FL-HSPCs progressively

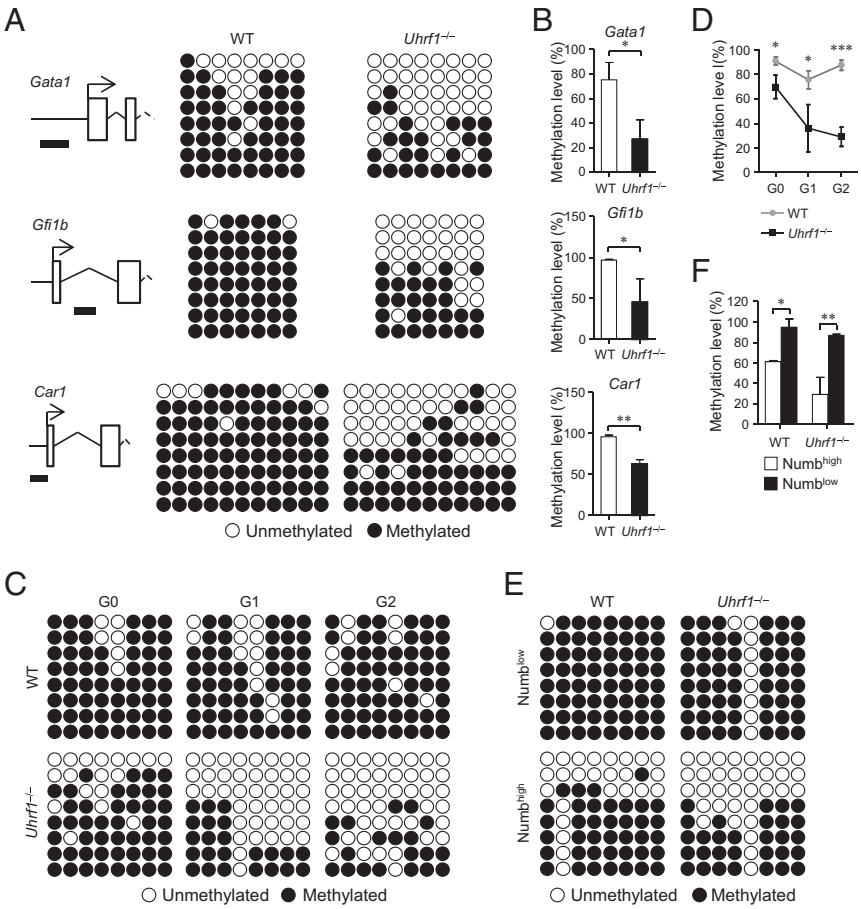

Fig. 5. The DNA methylation patterns of erythroid-specific genes are impaired during FL-HSC division in the absence of Uhrf1. (*A* and *B*) Methylation analysis of selected erythroid-specific genes (*Gata1*, *Gfi1b*, *Car1*) was performed by bisulfite conversion of genomic DNA extracted from FACS sorted control and Uhrf1-deficient FL-HSPCs (LSKs) at 13.5 dpc ($n = 3$). (*A*) The relative positions of the selected CpG sites in each gene (*Left*) and clonal bisulfite sequencing results (*Right*) are shown. (*B*) The methylation levels of the selected genes in *A*. (*C* and *D*) Clonal bisulfite sequencing results (*C*) and methylation levels (*D*) of the *Gata1* promoter in sorted 12.5-dpc control and Uhrf1-deficient FL-HSPCs (LSKs) after the indicated times of divisions. G0: generation 0; G1: generation 1; G2: generation 2 ($n = 3$). (*E* and *F*) Clonal bisulfite sequencing results (*E*) and methylation levels (*F*) of the *Gata1* promoter in Numb^{low} (stem-like) and Numb^{high} (committed) progenies from sorted control and Uhrf1-deficient FL-HSPCs (LSKs) after single division, as in Fig. 3 *D*, $^{**}P < 0.01$, $^{***}P < 0.001$ by Student's *t* test.

decreased through each generation, whereas it remained roughly unchanged in normal FL-HSPCs (Fig. 5 *C* and *D*).

Considering that Uhrf1 ablation impairs the balanced cell-division mode (Fig. 3 *D*–*F*) and abolishes the maintenance of DNA methylation imprints of erythroid-specific genes in FL-HSPCs, we sought to explore the relationship between Uhrf1-mediated DNA methylation and HSC-division mode. To this end, *Gata1* methylation level was analyzed in FACS-sorted Numb^{high} daughter cells and Numb^{low} daughter cells after single-round division. Interestingly, the DNA methylation level of *Gata1* in Numb^{low} daughter cells was significantly higher than those in Numb^{high} daughter cells in both WT and Uhrf1-deficient FL-HSPCs (Fig. 5 *E* and *F*), suggesting that Uhrf1 coordinates the HSC-division mode with the DNA methylation patterns of erythroid-specific genes. Taken together, the aforementioned data suggested that Uhrf1 establishes the DNA methylation patterns of erythroid-specific genes, which balances the HSC-division modes, therefore ensuring the precise cell fate decision of FL-HSCs.

Uhrf1 Controls the Self-Renewal Versus Differentiation of Adult HSCs. To further explore whether Uhrf1 serves similar functions in controlling the self-renewal versus differentiation and the cell-division modes of adult HSCs, we bred conditional Uhrf1$^{L/L}$ mice with the inducible *Mx1-cre* strain to ablate Uhrf1 in adult HSCs after poly(I:C) administration. The survival capacity of *Mx1-cre*$^{+}$Uhrf1$^{L/L}$ mice (designated Uhrf1^{KO} mice) was significantly reduced compared with that of *Mx1-cre*$^{-}$Uhrf1$^{L/L}$ mice (designated WT mice) (Fig. 6*A*), a result consistent with the significantly lower hematopoietic lineages and HSPCs in Uhrf1^{KO} mice (Fig. S6 *A*–*C*). Notably, flow cytometric analysis performed on day 13 after low-dosage poly(I:C) injection, when Uhrf1 had been efficiently ablated from HSPCs (Fig. S1 *E* and *F*), showed that both HPC(LK)s and HSCs (CD150^{+} CD34^{-} CD48^{-} LSKs) in Uhrf1^{KO} mice were dramatically reduced compared with those in WT mice (Fig. 6 *B* and *C* and Fig. S2 *B* and *C*).

CFU assays and competitive bone marrow transplantations (Fig. S6*D*) were then performed to evaluate the self-renewal capacity of Uhrf1-deficient adult HSCs. Compared with control HSPCs, Uhrf1-deficient HSPCs formed more BFU-E colonies but fewer CFU-GEMM and CFU-GM/G/M colonies (Fig. 6*D*). Consistently, Uhrf1-deficient adult HSCs failed to achieve multilineage reconstitution in irradiated mice compared with WT adult HSCs (Fig. 6 *E* and *F* and Fig. S6 *E* and *F*). Moreover, the HSC pool was not maintained after poly(I:C) administration (Fig. 6 *G* and *H*). Similarly to Uhrf1-dificient FL-HSCs, adult HSCs (CD150^{+} CD48^{-} LSKs) from Uhrf1^{KO} mice displayed impaired self-renewal capacity and were more prone to undergoing erythroid-biased differentiation compared with that in WT controls (Fig. 6 *I*–*L*). Moreover, adult HSCs from Uhrf1^{KO} mice underwent significantly fewer SS divisions (23.61% ± 11.51% vs. 45.29% ± 7.21% in WT

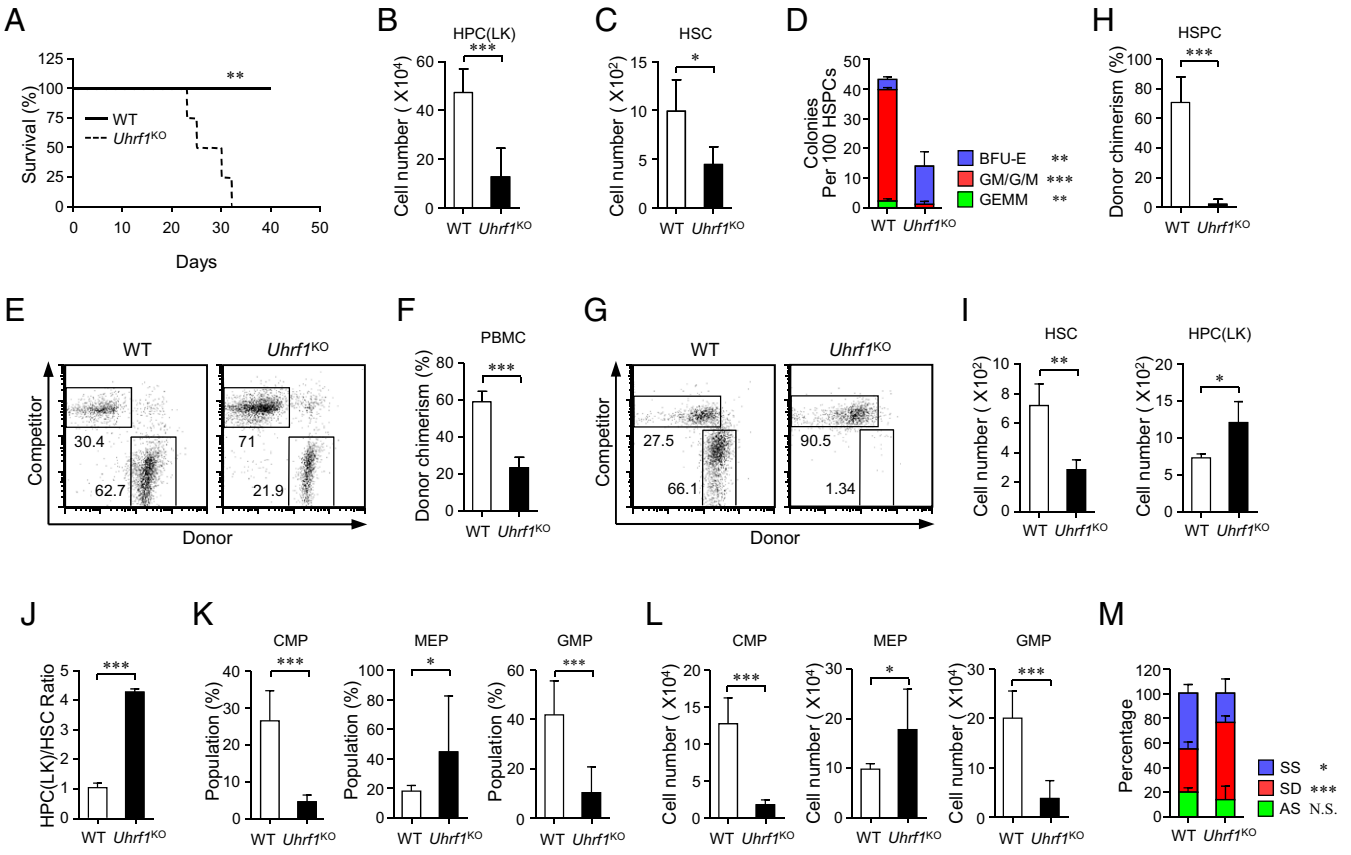

Fig. 6. Uhrf1 regulates the self-renewal versus differentiation of adult HSCs. (*A*) Kaplan–Meier survival curve of *Mx1-cre*$^{-}$Uhrf1$^{L/L}$ (WT, $n = 5$) and *Mx1-cre*$^{+}$Uhrf1$^{L/L}$ (Uhrf1^{KO}, $n = 4$) mice injected with poly(I:C). (*B* and *C*) Absolute cell numbers of HPC(LK)s (*B*) and HSCs (CD150^{+} CD34^{-} CD48^{-} LSKs) (*C*) from WT and Uhrf1^{KO} bone marrow 13 d after poly(I:C) injection. (*D*) Numbers of multilineage colonies (CFU-GEMM), erythroid colonies (BFU-E), and myeloid colonies (CFU-GM/G/M) generated by 100 HSPCs (LSKs) sorted from control and Uhrf1-deficient bone marrows 10 d after poly(I:C) injection. ($n = 4$). (*E* and *F*) Representative dot plots (*E*) and donor chimerism (*F*) of PBMCs in recipients transplanted as described in Fig. S6*D* ($n = 5$). (*G* and *H*) Representative dot plots (*G*) and donor chimerism (*H*) of HSPCs (LSKs) in recipients transplanted as described in Fig. S6*D* ($n = 5$). (*I* and *J*) Analysis of the self-renewal capacity of adult HSCs in culture. Sorted HSCs (CD150^{+} CD48^{-} LSKs) from WT or Uhrf1^{KO} bone marrow samples were cultured for 42 h before flow cytometric analysis. (*I*) Absolute numbers of HSCs and HPC(LK)s yielded by WT or Uhrf1^{KO} HSCs in culture. (*J*) The ratios of HPC(LK)s related to HSCs are shown ($n = 4$). (*K*) Percentages of CMPs, MEPs, and GMPs in WT and Uhrf1^{KO} bone marrow samples 10 d after poly(I:C) injection (WT, $n = 10$; Uhrf1^{KO}, $n = 9$). (*L*) Absolute cell numbers of CMPs, MEPs, and GMPs in WT and Uhrf1^{KO} bone marrow 10 d after poly(I:C) injection ($n = 5$). (*M*) Cell-division mode of WT and Uhrf1^{KO} HSCs (CD150^{+} CD48^{-} LSKs) ($n = 259$ (WT) or 134 (Uhrf1^{KO}) cell doublets from four independent experiments). The data are means ± standard deviation, for all panels: *$P < 0.05$, **$P < 0.01$, ***$P < 0.001$ by Student's *t* test; N.S.: no significance.

HSCs) and more SD divisions (62.56% ± 5.36% vs. 34.81% ± 5.78% in WT HSCs) (Fig. 6*M*). These data suggested that Uhrf1 serves conserved functions to control the self-renewal versus differentiation of adult HSCs through regulating the HSC-division modes.

Uhrf1 Controls the Cell Fate Decision of Adult HSCs Through Epigenetically Regulating the HSC-Division Modes. To further investigate whether adult HSCs use similar molecular mechanisms to control the decision of self-renewal versus differentiation, the expression of erythroid-specific genes was assessed in adult HSCs. Erythroid-specific genes were consistently up-regulated in Uhrf1-deficient adult HSCs compared with WT controls, whereas the stemness gene *Id2* was down-regulated (Fig. 7*A*). Moreover, bisulfite sequencing revealed that the DNA methylation of *Gata1* was significantly decreased in Uhrf1-deficient adult HSCs compared with WT controls (Fig. 7 *B* and *C*). These data indicated that adult HSCs use the conserved epigenetic regulation conducted by Uhrf1 to ensure precise cell fate decision.

Finally, retrovirus-mediated overexpression of Gata1 in adult HSCs was performed to determine whether the enhanced expression of erythroid-specific genes observed in Uhrf1-deficient HSCs accounts for the imbalanced cell-division mode and the subsequent increased differentiation commitment. Consistent with previous research (9), Gata1-overexpressing HSPCs formed more BFU-E colonies but fewer CFU-GEMM and CFU-GM/G/M colonies compared with vector transduced HSPCs in CFU assays (Fig. 7*D*), and Gata1-overexpressing HSCs did not achieve multilineage reconstitution in irradiated mice (Fig. 7 *E* and *F* and Fig. S6*G*). Notably, Gata1-overexpressing HSCs underwent fewer SS divisions (20.49% ± 5.37% vs. 56.35% ± 9.01% in vector transduced HSCs) and more SD divisions (61.70% ± 13.32% vs. 28.69% ± 8.75% in vector transduced HSCs) (Fig. 7*G*), which eventually led to increased differentiation of HSCs (Fig. 7*H*); thus, Gata1-overexpressing in HSCs is sufficient to phenocopy the Uhrf1-deficient HSCs. Altogether, we concluded that Uhrf1 controls the decision of self-renewal versus differentiation of HSCs through epigenetically regulating the HSC-division modes.

Discussion

The mechanism by which HSCs decide between self-renewal and differentiation is a long-standing question in the field. Here, we show that Uhrf1 is a bona fide epigenetic regulator that controls the self-renewal versus differentiation of HSCs. Uhrf1 epigenetically represses the expression of differentiation-promoting genes during division, which in turn balances the HSC-division modes, and thus controls the decision of self-renewal versus differentiation of HSCs.

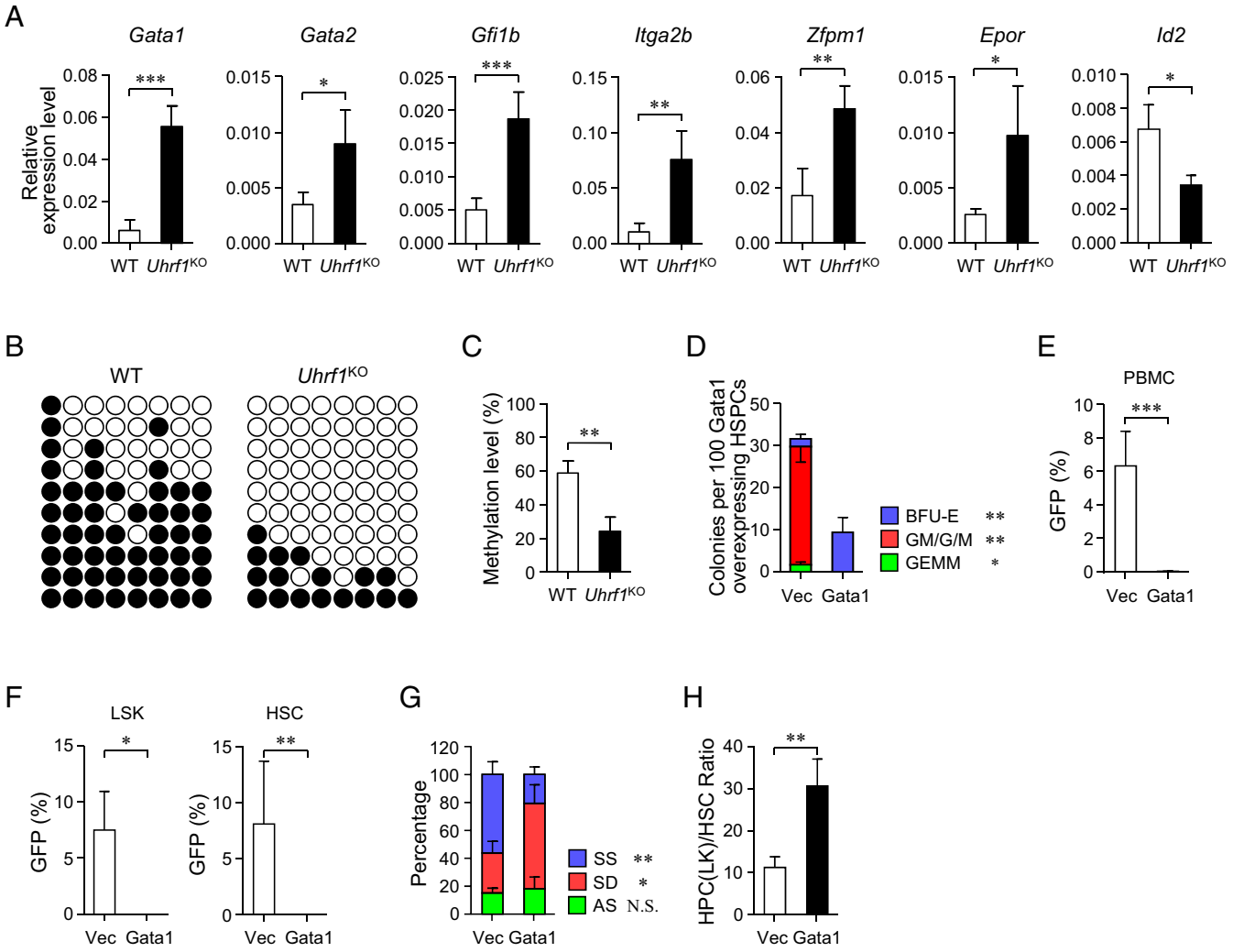

Fig. 7. Uhrf1 controls the cell fate decision of adult HSCs through epigenetically regulating HSC-division modes. (*A*) The transcriptional levels of representative erythroid-specific genes and stemness gene *Id2* in HSCs ($CD150^+$ $CD48^-$ LSKs) from WT and $Uhrf1^{KO}$ bone marrow samples ($n = 4$). (*B* and *C*) Clonal bisulfite sequencing results (*B*) and methylation levels (*C*) of the *Gata1* promoter in HSCs ($CD150^+$ $CD48^-$ LSKs) from WT and $Uhrf1^{KO}$ bone marrow samples ($n = 3$). (*D*) CFU assays of Gata1-overexpressing HSCs. Sorted HSCs ($CD150^+$ $CD48^-$ LSKs) from WT bone marrows were transduced with vector or *Gata1* cDNA and cultured for 36 h. One-hundred FACS-sorted transduced HSPCs (GFP^+ LSKs) were then seeded to the MethoCult media. Numbers of multilineage colonies (CFU-GEMM), erythroid colonies (BFU-E), and myeloid colonies (CFU-GM/G/M) were counted at day 8 ($n = 3$). (*E*) Percentages of donor chimerism of PBMCs (4 wk) in recipients transplanted with 200 sorted transduced HSCs (GFP^+ $CD150^+$ $CD48^-$ LSKs) together with 500,000 competitor bone marrow cells (vector, $n = 7$; Gata1, $n = 6$). (*F*) Percentages of donor chimerism of HSPCs (LSKs; 4 wk) and HSCs ($CD150^+$ $CD48^-$ LSKs; 4 wk) in recipients transplanted as described above (vector, $n = 7$; Gata1, $n = 6$). (*G*) Cell-division mode of HSCs ($CD150^+$ $CD48^-$ LSKs) transduced with a Gata1-overexpressing construct or vector ($n = 44$ (vector) or 61 (Gata1-overexpressing construct) cell doublets from three independent experiments). (*H*) Analysis of the self-renewal capacity of Gata1-overexpressing HSCs in culture. Sorted HSCs ($CD150^+$ $CD48^-$ LSKs) from WT bone marrows were transduced with vector or *Gata1* cDNA and cultured for 48 h. FACS-sorted transduced HSCs (GFP^+ $CD150^+$ $CD48^-$ LSKs) were then cultured for another 42 h before flow cytometric analysis. The ratio of HPC(LK)s related to HSCs is shown ($n = 3$). The data are means ± standard deviation, for all panels: $^*P < 0.05$, $^{**}P < 0.01$, $^{***}P < 0.001$ by Student's *t* test; N.S.: no significance.

Uhrf1 has been reported to regulate the survival and proliferation of cancer cells and invariant natural killer T cells (25, 33, 34); however, Uhrf1-deficient HSCs display normal survival and proliferation compared with WT HSCs. Intriguingly, Uhrf1-deficient HSCs undergo significantly more SD divisions at the expense of SS divisions, which is correlated with the enhanced expression of erythroid-specific genes. These findings emphasize that Uhrf1 specifically regulates the decision of self-renewal versus differentiation rather than other cell fate decision of HSCs.

The cell fate decision is regulated by both cell-intrinsic and cell-extrinsic mechanisms in various cell types (35–37), among which epigenetic regulation is the only heritable mechanism that controls stem cell fate (38, 39). As one of the epigenetic modifications, DNA methylation has been reported to maintain HSC self-renewal capacity (13, 40, 41). The present study supports this theory by highlighting that Uhrf1-mediated DNA methylation controls the self-renewal versus differentiation of individual HSC through epigenetically regulating the HSC-division modes. Our study highlights the possibility that the methylation level of certain key differentiation-promoting genes (such as *Gata1*) contributes to determining the HSC-division mode (choices among SS, SD, and AS). Briefly, HSCs that contain a high-methylation level of these genes (express low level of these genes) prefer undergoing SS division, whereas HSCs that harbor a low-methylation level are forced to undergo SD division, with the HSCs containing a medium-methylation level undergoing AS division. Further efforts should be made to address this hypothesis by using genetic models

that are able to quantitatively fine-tune the DNA methylation level of certain key differentiation-promoting genes.

FL-HSCs and adult HSCs differ in terms of cell-cycle dynamics, surface-marker expression, differentiation potential, and gene-expression profile (42–45). FL-HSCs and adult HSCs might use different mechanisms to control self-renewal and differentiation. Thus far, it has been reported that multiple factors serve different functions in fetal and adult HSCs. *Pten*, *Bmi1*, and *Cebpa* are required for adult HSC maintenance (46–48), whereas *Sox17*, *Ezh2*, and *Hmga2* regulate the self-renewal potential in fetal HSCs but not adult HSCs (8, 49, 50). In the current study, we not only identified Uhrf1 as a key factor that controls the self-renewal versus differentiation of FL-HSCs, but also extended the functions of Uhrf1 to adult HSCs, which use similar mechanisms as FL-HSCs. Therefore, Uhrf1-mediated DNA methylation and the coordinated cell-division modes have conserved functions in hematopoiesis throughout the lifespan.

Maintaining the balance between self-renewal and differentiation is a critical feature of HSCs, whereas aberrant balance can be a hallmark of oncogenesis (51). Leukemic stem cells (LSCs), which possess extensive self-renewal properties and have the capacity to undergo limited differentiation into leukemic blasts, are critical for the initiation and progression of all types of leukemia. Therefore, investigating the molecular wiring of LSCs is important because it may be possible to cure leukemia by targeting LSCs (52, 53). Previous research has identified Uhrf1 as an oncogene in various types of cancers, and the hypomethylation of the global genome driven by Uhrf1 overexpression contributes to cancer initiation and progression (33, 54, 55). In this study, our findings uncovered the vital functions of Uhrf1 in regulating the self-renewal versus differentiation of HSCs through epigenetically regulating their division patterns. The conserved functions of Uhrf1 in both fetal liver and adult HSCs raise the possibility that Uhrf1 may play a role in maintaining LSC self-renewal. Further investigations should be conducted to elucidate the underlying mechanisms and to determine whether Uhrf1 can serve as a potential target for defining new approaches to leukemia therapy.

Materials and Methods

Mice. The Uhrf1 floxed mice were obtained as described previously (25). The *Mx1-cre* mice (strain: B6.Cg-Tg(Mx1-cre)1Cgn/J), the *Vav1-cre* transgenic mice (strain: B6.Cg-Tg(Vav1-cre)A2Kio/J), and CD45.1 mice (strain: B6.SJL-*Ptprc*^{a}*Pepc*^{b}/BoyJ) were obtained from The Jackson Laboratory. All mice were bred and housed in specific pathogen-free conditions. The experimental embryos were generated by crossing Uhrf1$^{L/L}$ mice with *Vav1-cre*$^{+}$Uhrf1$^{L/+}$ mice. *Mx1-cre*–induced gene deletion was done by intraperitoneal injection of poly(I:C) (300 μg per mice) four times at 2-d intervals. For low-dosage poly(I:C) administration, mice were intraperitoneally injected with poly(I:C) (100 μg per mice) three times at 2-d intervals. All mice were genotyped using PCR analysis before experimentation (primer pairs for genotyping are listed in Table S2). All animal experiments were approved by the Institutional Animal Care and Use Committee of the Shanghai Institutes for Biological Sciences, Chinese Academy of Sciences.

Cell Culture and Methylcellulose Colony Formation Assay. Unless indicated, sorted FL-HSCs, FL-HSPCs, and adult HSCs were seeded into a 96-well U-bottom plate in IMDM supplemented with 10% (vol/vol) fetal bovine serum (FBS), 50 μM 2-mercaptoethanol, 100 IU/mL penicillin, and 100 μg/mL streptomycin (Gibco), SCF (50 ng/mL), murine interleukin-3 (mIL-3; 10 ng/mL) and murine interleukin-6 (mIL-6; 10 ng/mL). At indicated time points, cells were harvested and subjected to flow cytometric analysis. All cytokines were from PeproTech. For methylcellulose assays, 100 sorted FL-HSPCs (LSKs) were plated in duplicate in Iscove's modified medium-based methylcellulose medium (Methocult M3434, StemCell Technologies). Erythroid (BFU-E), myeloid (CFU-GM), and multilineage (CFU-GEMM) colonies were counted on day 8 or day 10.

BrdU Incorporation, Apoptosis Analysis, and CFSE Labeling. In vivo BrdU incorporation was performed as described previously (56). BrdU (100 mg/kg body weight; Sigma) was injected intraperitoneally into 13.5-dpc pregnant mice 2 h before killing the mice, then fetal livers were isolated from embryos. BrdU staining was performed using the APC BrdU Flow Kit (BD Pharmingen). Annexin V (Biolegend) and DAPI (Cell Signaling Technology) were used in apoptosis assays. In some experiments, fetal liver cells were stained with CFSE (5 μM; Sigma) and cultured overnight in IMDM supplemented with 10% (vol/vol) FBS, 50 μM 2-mercaptoethanol, antibiotics, TPO (10 ng/mL), and nocodazole (100 ng/mL; Sigma). CFSE^{+} FL-HSPCs (LSKs) were sorted and cultured for the indicated time points before analysis or FACS sorting.

Transplantation Assays. For FL-HSPC transplantation, 1,000 sorted FL-HSPCs (LSKs) (CD45.2^{+}) were transplanted into lethally radiated (10.8 Gy) recipient mice (CD45.1^{+}) along with 500,000 competitive bone marrow cells derived from nonirradiated recipient mice (CD45.1^{+}) by tail vein injection. Recipient mice received donor cells derived from one individual embryo of a given genotype. Peripheral blood of recipient mice was collected at 8 wk after transplantation. For comparative transplantation of adult HSCs, total bone marrow cells from CD45.1^{+} competitor and either CD45.2^{+} *Mx1-cre*$^{-}$Uhrf1$^{L/L}$ or CD45.2^{+} *Mx1-cre*$^{+}$Uhrf1$^{L/L}$ mice was mixed at a ratio of 1:1 and a total of 2,000,000 cells were injected intravenously into lethally radiated recipient mice. Uhrf1 deletion was achieved by poly(I:C) administration 4-wk post-transplantation and donor chimerism was assessed 4 wk after Uhrf1 deletion. For comparative transplantation of Gata1-overexpressing HSCs, 200 sorted transduced HSCs (GFP^{+} CD150^{+} CD48^{-} LSKs) together with 500,000 competitor bone marrow cells were injected intravenously into lethally radiated recipient mice.

Cell Isolation, FACS Analysis, and Cell Sorting. Fetal livers were isolated from experimental embryos at the indicated gestational age. Single-cell suspensions were prepared by triturating with IMDM (Gibco) supplemented with 10% (vol/vol) FBS (HyClone), then filtering through nylon screen (40 μM; BD Biosciences). Bone marrow cells were obtained by flushing tibias and femurs from experimental mice, followed by red blood cell lysis before filtration. Surface staining was carried out as described previously (57). The following antibodies were used to define lineage^{+} cells: anti-CD3e (145-2C11), anti-CD4 (GK1.5), anti-CD8 (53-6.7), anti-Gr1 (RB6-8C5), anti-TER119 (TER119), and anti-B220 (RA3-6B2). The following additional antibodies were used to define FL-HSCs (CD150^{+} CD48^{-} Mac1^{low} LSKs), FL-HSPCs (LSKs), HPCs(LKs), and AGM-HSCs: anti-cKit (2B8), anti-Sca1 (D7), anti-CD48 (HM48-1), anti-CD150 (TC15-12F12.2), anti-Mac1 (M1/70), and anti-CD34 (RAM34). For identifying adult HSCs, anti-Mac1 (M1/70) was added to the lineage mixture. For identifying CMPs, GMPs, and MEPs, anti-CD16/32 (93) were used. To measure donor-derived chimerism, peripheral blood from recipients was obtained by the tail vein-bleeding method and prepared as previously described (58), the following antibodies were used to assess multilineage reconstitution: anti-CD3e (145-2C11), anti-B220 (RA3-6B2), anti-Gr1 (RB6-8C5), anti-Mac1 (M1/70), anti-CD45.1 (A20), and anti-CD45.2 (104). All antibodies were from BD Pharmingen, Biolegend, and eBioscience. Cell fluorescence was acquired on a four-laser BD LSRFortessa II or a two-laser BD FACSCalibur and was analyzed with FlowJo software. Cell sorting was carried by a BD FACSAria II after surface staining. Sorted cell purity was over 90%.

Retroviral Production and Transduction. Mouse *Gata1* cDNAs were cloned into the pMCs-IRES-GFP retroviral vector. Virus was packaged in PlatE cell line and the viral supernatants were collected at 4 d after transfection. For retroviral transduction, freshly isolated whole fetal liver cells or 5-FU–treated whole bone marrow cells were suspended with retroviral supernatant in the presence of 8 μg/mL polybrene (Sigma) and then centrifuged at 1,500 × *g* for 2 h at 32 °C. Retroviral supernatants were then replaced by flesh culture medium after transduction.

Quantitative Real-Time PCR Analysis. Total RNA was extracted from FACS-sorted cells using the Quick-RNA MicroPrep Kit (Zymo Research), then reverse-transcribed with the HiScript II Q RT SuperMix for quantitative PCR (qPCR) (+gDNA wiper) Kit (Vazyme). Real-Time PCR was performed using SYBE Green Realtime PCR master Mix (TOYOBO) on a Rotor-Gene Q machine. β-Actin was used as internal control. The primer pairs for the genes examined are listed in Table S2.

Immunofluorescence Staining for Numb Distribution. Immunofluorescence staining for Numb distribution was performed as previously described (17). Briefly, sorted HSCs and HSPCs were stimulated in IMDM supplemented with 20% (vol/vol) BIT 9500 serum substitute (STEMCELL, 09500), 50 μM 2-mercaptoethanol, 50 ng/mL SCF, and 50 ng/mL TPO for 16 h then treated with 10 nM nocodazole for 24 h to arrest cells in late telophase. Cells were then harvested, fixed with 4% (vol/vol) paraformaldehyde, and settled on coverslips coated with poly-L-lysine (Sigma) at 37 °C for 1 h. Cells were permeabilized with 0.5% Triton X-100 and blocked with 1% BSA in Tris-Buffered Saline and Tween 20 (TBST). Coverslips were stained overnight at 4 °C with antibody against Numb (1:100; ABcam, ab14140) diluted in blocking buffer. Primary antibody staining was developed with secondary antibody conjugated to FITC together with DAPI (1 μg/mL). Slides were analyzed on a Leica confocal microscope. ImageJ software was used to determine fluorescence intensity of pixels following staining for Numb.

Western Blot Analysis. Cell lysates from WT (*Uhrf1*$^{fl/+}$ or *Uhrf1*$^{fl/fl}$) and Uhrf1-deficient lineage$^-$ cKit$^+$ cells were separated by SDS/PAGE. Proteins were detected by antibodies against Uhrf1 (mouse polyclonal, generated in our own laboratory) or β-actin (Sigma, A1978). First antibodies were developed by HRP-conjugated goat anti-mouse IgG1 (Santa Cruz, sc-2005).

RNA-seq, Library Generation, and Bioinformatics Analysis. FL-HSPCs (LSKs) (~10,000 cells) were isolated from WT and Uhrf1$^{-/-}$ fetal livers by cell sorting (double sort, purity > 95%). RNA was extracted, purified, and checked for integrity using an Agilent Bioanalyzer 2100 (Agilent Technologies). Libraries were generated for sequencing using the TruSeq RNA sample preparation kit (Illumina). Libraries were sequenced using an Illumina HiSEq. 2500 sequencer. All of the above processes were performed at Shanghai Biotechnology Corporation, Shanghai, China. For GO enrichment analysis, selected differentially regulated genes between WT and Uhrf1$^{-/-}$ FL-HSPCs (LSKs) with a Fisher-test–corrected $P < 0.05$ were analyzed on the Gene Ontology Consortium website (geneontology.org). All data are representative of three independent experiments. The accession number for the RNA-seq data reported in this report is GEO no. GSE85450.

Bisulfite Sequencing and Global DNA Methylation Analysis. Bisulfite sequencing was started with 2,000 sorted cells and converted with the EZ DNA Methylation-Direct Kit (Zymo Research). Selected genomic regions were PCR-amplified by Taq HS enzyme (Takara). The PCR products were gel-purified using the Gel Extraction Kit (Qiagen) and then cloned into pMD 18-T vector (Takara) for sequencing. Data were analyzed online using BISMA (services.ibc.uni-stuttgart.de/BDPC/BISMA/). Global DNA methylation analysis was performed using the 5-mC DNA ELISA Kit (Zymo research) according to the manufacturer's instructions.

Statistical Analysis. Unless indicated, all experiments showed were performed at least three times. All data are expressed as means ± SD and two-tailed unpaired Student's *t* test were used to determine statistical significance. For all experiments: $*P < 0.05$, $**P < 0.001$, $***P < 0.0001$.

ACKNOWLEDGMENTS. We thank Baojin Wu and Guoyuan Chen for the animal husbandry, and Wei Bian for the support of cell sorting. This work was supported by the National Basic Research Program of China (Grant 2013CB835300), the National Natural Science Foundation of China (Grants 31530021 and 31501193), the Strategic Priority Research Program of the Chinese Academy of Sciences (Grant XDB19000000), and the China Postdoctoral Science Foundation (Grant 2015M581672).

1. Bryder D, Rossi DJ, Weissman IL (2006) Hematopoietic stem cells: The paradigmatic tissue-specific stem cell. *Am J Pathol* 169(2):338–346.
2. Eaves CJ (2015) Hematopoietic stem cells: Concepts, definitions, and the new reality. *Blood* 125(17):2605–2613.
3. Rönnstrand L (2004) Signal transduction via the stem cell factor receptor/c-Kit. *Cell Mol Life Sci* 61(19-20):2535–2548.
4. Duncan AW, et al. (2005) Integration of Notch and Wnt signaling in hematopoietic stem cell maintenance. *Nat Immunol* 6(3):314–322.
5. Luis TC, et al. (2011) Canonical wnt signaling regulates hematopoiesis in a dosage-dependent fashion. *Cell Stem Cell* 9(4):345–356.
6. van Galen P, et al. (2014) Reduced lymphoid lineage priming promotes human hematopoietic stem cell expansion. *Cell Stem Cell* 14(1):94–106.
7. Lawrence HJ, et al. (2005) Loss of expression of the Hoxa-9 homeobox gene impairs the proliferation and repopulating ability of hematopoietic stem cells. *Blood* 106(12):3988–3994.
8. Copley MR, et al. (2013) The Lin28b-let-7-Hmga2 axis determines the higher self-renewal potential of fetal haematopoietic stem cells. *Nat Cell Biol* 15(8):916–925.
9. Iwasaki H, et al. (2003) GATA-1 converts lymphoid and myelomonocytic progenitors into the megakaryocyte/erythrocyte lineages. *Immunity* 19(3):451–462.
10. Randrianarison-Huetz V, et al. (2010) Gfi-1B controls human erythroid and megakaryocytic differentiation by regulating TGF-beta signaling at the bipotent erythro-megakaryocytic progenitor stage. *Blood* 115(14):2784–2795.
11. Trowbridge JJ, Snow JW, Kim J, Orkin SH (2009) DNA methyltransferase 1 is essential for and uniquely regulates hematopoietic stem and progenitor cells. *Cell Stem Cell* 5(4):442–449.
12. Bröske AM, et al. (2009) DNA methylation protects hematopoietic stem cell multipotency from myeloerythroid restriction. *Nat Genet* 41(11):1207–1215.
13. Challen GA, et al. (2014) Dnmt3a and Dnmt3b have overlapping and distinct functions in hematopoietic stem cells. *Cell Stem Cell* 15(3):350–364.
14. Yanai T, et al. (1995) Separate control of the survival, the self-renewal and the differentiation of hemopoietic stem cells. *Cell Struct Funct* 20(2):117–124.
15. Morrison SJ, Kimble J (2006) Asymmetric and symmetric stem-cell divisions in development and cancer. *Nature* 441(7097):1068–1074.
16. Wu M, et al. (2007) Imaging hematopoietic precursor division in real time. *Cell Stem Cell* 1(5):541–554.
17. Will B, et al. (2013) Satb1 regulates the self-renewal of hematopoietic stem cells by promoting quiescence and repressing differentiation commitment. *Nat Immunol* 14(5):437–445.
18. Wilson A, et al. (2004) c-Myc controls the balance between hematopoietic stem cell self-renewal and differentiation. *Genes Dev* 18(22):2747–2763.
19. Bostick M, et al. (2007) UHRF1 plays a role in maintaining DNA methylation in mammalian cells. *Science* 317(5845):1760–1764.
20. Xie S, Jakoncic J, Qian C (2012) UHRF1 double Tudor domain and the adjacent PHD finger act together to recognize K9me3-containing histone H3 tail. *J Mol Biol* 415(2):318–328.
21. Du J, Johnson LM, Jacobsen SE, Patel DJ (2015) DNA methylation pathways and their crosstalk with histone methylation. *Nat Rev Mol Cell Biol* 16(9):519–532.
22. Sharif J, et al. (2007) The SRA protein Np95 mediates epigenetic inheritance by recruiting Dnmt1 to methylated DNA. *Nature* 450(7171):908–912.
23. Hashimoto H, et al. (2008) The SRA domain of UHRF1 flips 5-methylcytosine out of the DNA helix. *Nature* 455(7214):826–829.
24. Obata Y, et al. (2014) The epigenetic regulator Uhrf1 facilitates the proliferation and maturation of colonic regulatory T cells. *Nat Immunol* 15(6):571–579.
25. Cui Y, et al. (2016) Uhrf1 controls iNKT cell survival and differentiation through the Akt-mTOR axis. *Cell Reports* 15(2):256–263.
26. Kim I, He S, Yilmaz OH, Kiel MJ, Morrison SJ (2006) Enhanced purification of fetal liver hematopoietic stem cells using SLAM family receptors. *Blood* 108(2):737–744.
27. Dzierzak E, Speck NA (2008) Of lineage and legacy: The development of mammalian hematopoietic stem cells. *Nat Immunol* 9(2):129–136.
28. Takizawa H, Regoes RR, Boddupalli CS, Bonhoeffer S, Manz MG (2011) Dynamic variation in cycling of hematopoietic stem cells in steady state and inflammation. *J Exp Med* 208(2):273–284.
29. Sanjuan-Pla A, et al. (2013) Platelet-biased stem cells reside at the apex of the haematopoietic stem-cell hierarchy. *Nature* 502(7470):232–236.
30. Krivtsov AV, et al. (2006) Transformation from committed progenitor to leukaemia stem cell initiated by MLL-AF9. *Nature* 442(7104):818–822.
31. Liu B, et al. (2014) PIAS1 SUMO ligase regulates the self-renewal and differentiation of hematopoietic stem cells. *EMBO J* 33(2):101–113.
32. Jones PA (2012) Functions of DNA methylation: Islands, start sites, gene bodies and beyond. *Nat Rev Genet* 13(7):484–492.
33. Wang F, et al. (2012) UHRF1 promotes cell growth and metastasis through repression of p16(ink^{4}a) in colorectal cancer. *Ann Surg Oncol* 19(8):2753–2762.
34. Jenkins Y, et al. (2005) Critical role of the ubiquitin ligase activity of UHRF1, a nuclear RING finger protein, in tumor cell growth. *Mol Biol Cell* 16(12):5621–5629.
35. Dumont NA, Wang YX, Rudnicki MA (2015) Intrinsic and extrinsic mechanisms regulating satellite cell function. *Development* 142(9):1572–1581.
36. Cayouette M, Barres BA, Raff M (2003) Importance of intrinsic mechanisms in cell fate decisions in the developing rat retina. *Neuron* 40(5):897–904.
37. Zon LI (2008) Intrinsic and extrinsic control of haematopoietic stem-cell self-renewal. *Nature* 453(7193):306–313.
38. Lunyak VV, Rosenfeld MG (2008) Epigenetic regulation of stem cell fate. *Hum Mol Genet* 17(R1):R28–R36.
39. Jaenisch R, Bird A (2003) Epigenetic regulation of gene expression: How the genome integrates intrinsic and environmental signals. *Nat Genet* 33(Suppl):245–254.
40. Sun D, et al. (2014) Epigenomic profiling of young and aged HSCs reveals concerted changes during aging that reinforce self-renewal. *Cell Stem Cell* 14(5):673–688.
41. Moran-Crusio K, et al. (2011) Tet2 loss leads to increased hematopoietic stem cell self-renewal and myeloid transformation. *Cancer Cell* 20(1):11–24.
42. Pietras EM, Warr MR, Passegué E (2011) Cell cycle regulation in hematopoietic stem cells. *J Cell Biol* 195(5):709–720.
43. Mikkola HK, Orkin SH (2006) The journey of developing hematopoietic stem cells. *Development* 133(19):3733–3744.
44. Orkin SH, Zon LI (2008) Hematopoiesis: An evolving paradigm for stem cell biology. *Cell* 132(4):631–644.
45. Chen X, et al. (2014) Lis1 is required for the expansion of hematopoietic stem cells in the fetal liver. *Cell Res* 24(8):1013–1016.
46. Zhang J, et al. (2006) PTEN maintains haematopoietic stem cells and acts in lineage choice and leukaemia prevention. *Nature* 441(7092):518–522.
47. Park IK, et al. (2003) Bmi-1 is required for maintenance of adult self-renewing haematopoietic stem cells. *Nature* 423(6937):302–305.
48. Ye M, et al. (2013) C/EBPa controls acquisition and maintenance of adult haematopoietic stem cell quiescence. *Nat Cell Biol* 15(4):385–394.
49. He S, Kim I, Lim MS, Morrison SJ (2011) Sox17 expression confers self-renewal potential and fetal stem cell characteristics upon adult hematopoietic progenitors. *Genes Dev* 25(15):1613–1627.
50. Mochizuki-Kashio M, et al. (2011) Dependency on the polycomb gene Ezh2 distinguishes fetal from adult hematopoietic stem cells. *Blood* 118(25):6553–6561.
51. Tan BT, Park CY, Ailles LE, Weissman IL (2006) The cancer stem cell hypothesis: A work in progress. *Lab Invest* 86(12):1203–1207.
52. Horton SJ, Huntly BJ (2012) Recent advances in acute myeloid leukemia stem cell biology. *Haematologica* 97(7):966–974.
53. Somervaille TC, Cleary ML (2006) Identification and characterization of leukemia stem cells in murine MLL-AF9 acute myeloid leukemia. *Cancer Cell* 10(4):257–268.
54. Jeanblanc M, et al. (2005) The retinoblastoma gene and its product are targeted by ICBP90: A key mechanism in the G1/S transition during the cell cycle. *Oncogene* 24(49):7337–7345.
55. Mudbhary R, et al. (2014) UHRF1 overexpression drives DNA hypomethylation and hepatocellular carcinoma. *Cancer Cell* 25(2):196–209.
56. Liu F, et al. (2010) FIP200 is required for the cell-autonomous maintenance of fetal hematopoietic stem cells. *Blood* 116(23):4806–4814.
57. Wang X, et al. (2008) Regulation of Tcrb recombination ordering by c-Fos-dependent RAG deposition. *Nat Immunol* 9(7):794–801.
58. Cheng H, Liang PH, Cheng T (2013) Mouse hematopoietic stem cell transplantation. *Methods Mol Biol* 976:25–35.